Published online July 5, 2018

Original Research

Core Ideas

- Cation exchange (CE) on illite, a main sorption process for Cs^+, is driven by Cs^+ concentration.
- Undefined CE and surface complexation on OM are main sorption processes for Sr^{2+}.
- $^{137}Cs^+$ migrated only into shallow depths of a few centimeters after 3 yr.
- $^{90}Sr^{2+}$ migrated into deeper layers of the soil due to competitive sorption.

Numerical and Experimental Investigations of Cesium and Strontium Sorption and Transport in Agricultural Soils

Anne E. Berns,* Alexander Flath, Khalid Mehmood, Diana Hofmann, Diederik Jacques, Martin Sauter, Harry Vereecken, and Irina Engelhardt

A process-based knowledge of the sorption mechanisms in soils is a prerequisite for the prediction of radionuclide transport in soils, plant availability, and leaching risk into groundwater. The present study combined batch sorption experiments of Cs^+ and Sr^{2+} in agricultural soils of differing soil texture with numerical experiments using PHREEQC to identify key processes of sorption at different temperatures. Sorption was simulated for both radionuclides using cation exchange models. In addition, surface complexation was integrated into the reaction network for Sr^{2+}. Our geochemical simulations identified cation exchange on illite as the dominant sorption process for Cs^+. Selection of the site types in Cs^+ sorption was mainly driven by Cs^+ concentration. At low Cs^+ concentrations the highly selective frayed edge sites dominated sorption behavior, while less affine site types on illite constituted the major sorption partners at high concentrations. We identified undefined cation exchange as the dominant sorption process for Sr^{2+}, followed by surface complexation on organic matter. These process-based analyses were the basis for field-scale simulations to predict the leaching risk of Cs and Sr radionuclides in agricultural soils under humid climate conditions. For both soils and radionuclides, the distribution coefficients (K_d) varied distinctly with time in shallow layers due to changes in temperature, saturation, and the prevailing dominant sorption processes. During a 3-yr-simulation period, $^{137}Cs^+$ migrated to depths of 3.6 cm (silty loam) and 7.6 cm (sandy loam), while $^{90}Sr^{2+}$ migrated to depths of 15.6 cm (silty loam) and 23.6 cm (sandy loam) due to competitive sorption of infiltrating Ca^{2+} and Mg^{2+} ions reducing $^{90}Sr^{2+}$ sorption and displacing $^{90}Sr^{2+}$ from its exchange sites.

Abbreviations: CEC, cation exchange capacity; CEC_{eff}, effective cation exchange capacity; CEC_{pot}, potential cation exchange capacity; FES, frayed edge sites; HFO, hydrous ferric oxides; OM, organic matter; RN, radionuclide; TOC, total organic carbon.

A.E. Berns, K. Mehmood, D. Hofmann, H. Vereecken, and I. Engelhardt, Agrosphere Institute (IBG-3), Forschungszentrum Jülich GmbH, Wilhelm-Johnen-Straße, 52425 Jülich, Germany; A. Flath, Geographisches Institut, Ruhr-Univ. Bochum, Universitätsstraße 150, 44780 Bochum, Germany; D. Jacques, Institute for Environment, Health and Safety, Belgian Nuclear Research Centre (SCK•CEN), Mol, Belgium; M. Sauter, Dep. of Applied Geology, Georg-August-Univ. Göttingen, Goldschmidt-Str. 3, 37077 Göttingen, Germany; I. Engelhardt, Chair for Hydrogeology, Technische Univ. Berlin, Ernst-Reuter-Platz 1, 10587 Berlin, Germany. *Corresponding author (a.berns@fz-juelich.de).

Received 19 June 2017.
Accepted 22 May 2018.
Supplemental material online.

Citation: Berns, A.E., A. Flath, K. Mehmood, D. Hofmann, D. Jacques, M. Sauter, H. Vereecken, and I. Engelhardt. 2018. Numerical and experimental investigations of cesium and strontium sorption and transport in agricultural soils. Vadose Zone J. 17:170126. doi:10.2136/vzj2017.06.0126

Environmental contamination by radionuclides (RNs) from localized nuclear fallout, such as those following the Chernobyl or Fukushima accidents, constitutes a threat to human health due to the emission of highly energetic radiation. Cesium-137 (half-life: 30 yr) and ^{90}Sr (half-life: 28 yr) are two of the most abundant and harmful radioisotopes emitted to the environment (UN Scientific Committee on the Effects of Atomic Radiation, 1996). During the last century, the Chernobyl fallout resulted in soil contamination of up to 40,000 kBq m^{-2} (Niedrée et al., 2013) in the vicinity of the reactor. In Belarus and Ukraine, ^{137}Cs accumulations of up to 20,000 kBq m^{-2} were measured (Kashparov et al., 2003). The less volatile ^{90}Sr was mainly deposited close to the reactor, and ^{90}Sr contamination of up to 10,000 kBq m^{-2} were measured in the 30-km zone (Kashparov et al., 2003).

Agricultural areas are most sensitive to RN contamination. The bioavailability of Cs^+ and Sr^{2+} is affected due to competitive sorption because the application of fertilizers alters the concentrations of major nutrients (e.g., K^+, Ca^{2+}, and Mg^{2+}) (Wang and Staunton, 2005). Hence, the application of organic amendments (e.g., compost, biochar, or digestate) can affect the mobility of Cs^+ and Sr^{2+}, e.g., due to the supply of competing

nutrients or an increase in sorption sites. Biochar and digestate, common byproducts of bioenergy production, are increasingly applied to agricultural soils (Novotny et al., 2015; Scotti et al., 2015). Both amendments affect organic matter (OM) content and ionic strength as well as soil pH (Van Bergeijk et al., 1992; Krouglov et al., 1997) and thus the bioavailability of Cs^+ and Sr^{2+} (Hamilton et al., 2016).

Cesium binds to negatively charged soil compounds via ion exchange and exhibits stronger sorption to clay minerals than to sesquioxides or OM (Cornell, 1993; Dumat and Staunton, 1999; Staunton and Levacic, 1999). Thus, due to an additional blocking of clay sorption sites by OM and the low tendency of Cs^+ to form organic complexes, Cs^+ sorption is usually low in OM-enriched soils (Sanchez et al., 1988; Ivanov et al., 1997). In contrast, Sr^{2+} strongly binds to OM via chelation and surface complexation, but sorption to clay minerals is limited due to reversible sorption processes (Sanchez et al., 1988; Van Bergeijk et al., 1992). Thus, in soils with a high content of OM (>2%) Sr^{2+} is preferentially retained, while in soils enriched with clay minerals, Sr^{2+} can migrate farther downward and possibly reach groundwater (Nilsson et al., 1985; Ivanov et al., 1997). Organic amendments such as biochars or digestate hence are expected to have an impact on sorption and transport behavior of the two RNs through a number of mechanisms. On the one hand, biochars could offer a larger number of OM-borne sorption sites, especially for Sr^{2+}, due to their large surface areas. On the other hand, biochars could reduce the number of sorption sites provided by clay minerals, especially for Cs^+, through blocking of smaller pores in the soil matrix and thereby blocking access to clay mineral sites within these. Because the charring process usually removes chemical structures containing oxygen, biochars are mostly composed of aromatic and aliphatic structures (de la Rosa et al., 2014), which are more resilient to microbial degradation (Kleber, 2010). Biochar amendment should hence have a lasting effect on the organic C content of the soils. Digestate amendment is also expected to introduce large amounts of OM, and the same considerations as for biochar apply. However, because the OM of digestates contains larger amounts of easily degradable structures like carbohydrates or proteins (Tambone et al., 2013), the OM of digestates is prone to microbial degradation. The addition of digestate OM should hence have less effect in the medium and long term than the addition of biochar. Digestate amendment also introduces larger amounts of nutrients, which can influence the sorption of the RNs through competitive sorption. Because those nutrients are usually very mobile in soil, their influence is expected to be only of short duration.

To predict the availability to plants, translocation, and the leaching risk of RNs in soil by numerical modeling, process-based knowledge of sorption mechanisms is required (Goldberg et al., 2007; Payne et al., 2013) because the quantification of soil–plant–human transfer flux requires the speciation of RNs (Skipperud and Salbu, 2015). Most numerical Cs^+ and Sr^{2+} sorption models were developed for the risk assessment of nuclear waste repository sites (Maes et al., 2012; Organisation for Economic Co-operation and Development/Nuclear Energy Agency, 2012; Piqué et al., 2013). After the Chernobyl accident, numerical models were applied to investigate the migration of $^{137}Cs^+$ and $^{90}Sr^{2+}$ in the grassland soil of northern Italy (Chamard et al., 1993), forest soil and bedrock in Finland (Lehto, 2015), and two different agricultural soils based on literature values (Hormann and Fischer, 2013). Furthermore, the transport of uranium through agricultural soils was investigated by Jacques et al. (2006) for nuclear repository siting in Belgium. The models performed reasonably well, but each of them was adapted to the problem at hand and neither of these numerical investigations of Cs^+ and Sr^{2+} behavior in soil encompassed sorption processes on both mineral as well as organic sorption sites. We believe that a model taking into account all sorption processes would allow a more detailed analysis of experimental data and could be applied to a larger range of nuclides.

The aims of this study were (i) to simulate the effects of cation exchange and surface complexation on soil OM on RN transport of Cs^+ and Sr^{2+} in soil and (ii) to assess the influence of soil texture (silty vs. sandy soil) and OM content as well as the medium-term impact of modern amendments like biochar and digestate on the RN transport in soil. We investigated the sorption behavior of Cs^+ and Sr^{2+} using standard batch experiments that were analyzed using PHREEQC to identify key processes of RN sorption. Two process-oriented models were implemented to investigate cation exchange mechanisms. For Sr^{2+}, additional conceptual models accounting for surface complexation on OM and on Fe- and Mn-oxide surfaces, i.e., a multisite complexation model, were implemented. We then used the completed mathematical model to predict the field-scale leaching risk of Cs and Sr radionuclides in agricultural soils under humid climatic conditions based on available lysimeter data.

Materials and Methods

Laboratory Experiments

Chemicals, Soils, and Organic Soil Amendments

Chemicals (CsCl, $SrCl_2 \cdot 6H_2O$, $CaCl_2 \cdot 2H_2O$, and $BaCl_2$) and triethanolamine were obtained from Merck (Germany) in analytical purity quality. All experiments were conducted with deionized water (conductivity <5 $\mu S\ cm^{-1}$).

Two soil types were used in this study: a silty loam (orthic Luvisol) and a sandy loam (gleyic Cambisol) from arable lands. Soil characteristics are provided in Table 1 (Berns et al., 2008; Garré et al., 2010; Kasteel et al., 2005). The soils were chosen for their differing mineral and organic compositions.

Biochar was produced from wood chips by slow pyrolysis (400–450°C; Carbon Terra GmbH). The chemical composition of this low-temperature biochar consisted only of aromatic structures, as was determined by ^{13}C solid-state nuclear magnetic resonance spectroscopy (Supplemental Fig. S1). The surface area was 231 $m^2\ g^{-1}$ and the organic C content was 75.9% (Mukherjee et al., 2016). The liquid fraction of a biogas digestate (i.e., the liquor) was obtained from an anaerobic digester operated under mesophilic

conditions (Schwalmtal, Germany; PlanET Biogastechnik GmbH). The daily feed rate for the digester was 50 t, consisting of 60% maize (*Zea mays* L.) silage, 4% chicken manure, 20% beef urine, and 16% pig urine (w/w, fresh content). The element analysis of the liquor was as follows: 6.51 g L^{-1} total N, 3.49 g L^{-1} NH_4–N, 3.21 g L^{-1} P, 6.17 g L^{-1} K, 1.51 g L^{-1} Mg, 2.04 g L^{-1} Ca, 1.3 g L^{-1} dissolved organic C.

Soil Preparation

Soil samples were collected from the plow horizon (0–25 cm below the surface), discarding crop residues like stubble or roots. The sieved arable soils (≤2 mm) were mixed with biochar and liquor according to common agricultural practice in North Rhine–Westphalia, Germany. Sieved biochar (≤2 mm) was added to the soils at a rate equivalent to 25 t ha^{-1} (i.e., 8.3 and 9.1 g kg^{-1} for the silty loam and sandy loam, respectively, on a dry mass basis). Liquor was added to the soils at 34 t ha^{-1} (i.e., 11.7 and 12.4 g kg^{-1} for the silty loam and sandy loam, respectively). All soils (treated and untreated) were incubated for 6 mo at temperatures between 5 and 15°C to get rid of easily degradable OM components and end up with stable soil–amendment mixtures that were resistant to OM degradation during the duration of the sorption experiments. Soil humidity was maintained at the respective initial field capacities by once a week replacing the water lost by evaporation, which was determined by weighing.

After incubation, relevant soil parameters were determined (in triplicate): pH, electrical conductivity, total organic C (TOC), total inorganic C, total N, cation exchange capacity (CEC), and plant-available nutrients (K^+, Ca^{2+}, and Mg^{2+}). Elemental analysis of total C and N was performed on milled soil samples (ball mill, Retsch) using a Vario EL cube (Elementar Analysensysteme GmbH) in CHN mode. Soil nutrients (K^+, Ca^{2+}, and Mg^{2+}) were extracted as described by Prost et al. (2013), and the extracts were analyzed by inductively coupled plasma–optical emission spectrometry (iCAP 6000, Thermo Scientific). The surface area of all soils was measured using an Autosorb 1 (Quantachrome GmbH and Co. KG) by applying the Brunauer–Emmett–Teller (BET) equation to multipoint N_2 adsorption isotherms at 343 K.

Sorption Batch Experiments

The soils were pre-equilibrated in $CaCl_2$ solutions to obtain a homogeneous distribution of Ca^{2+} on the sorption surfaces. Pre-equilibration was conducted in 50-mL polycarbonate centrifuge tubes (Nalgene) for Cs^+ and in 50-mL glass centrifuge tubes (Schott, Germany) for Sr^{2+}. Pre-equilibration was completed in three shaking and centrifugation steps with decreasing concentrations of 1, 0.1, and 0.01 M $CaCl_2$ (Organisation for Economic Co-operation and Development, 2000; Borchard et al., 2012) with 4 g of dry soil suspended in 20 mL of $CaCl_2$ solution (soil/solution rate 1:5 w/v).

Batch sorption experiments were performed in an incubator shaker G-25 (New Brunswick Scientific Co.) at 5 ± 1°C. Further experiments were conducted at 20 ± 2°C (on a benchtop horizontal shaker) and at 35 ± 1°C. The results of the latter are reported in the supplemental material. For all sorption experiments, a range of five concentration levels of CsCl and $SrCl_2$ (i.e., 0.1, 0.5, 1, 5, and 10 mM) was prepared. A 0.01 M $CaCl_2$ solution was used as the background electrolyte in all experiments. Following

Table 1. Characteristics of the soils used in this study.

Soil texture	Silty loam	Sandy loam
Soil group (FAO WRB)	orthic Luvisol	gleyic Cambisol
Location	Merzenhausen (NRW, Germany)	Kaldenkirchen (NRW, Germany)
Coordinates	50°55′50″ N, 6°17′50″ E	51°18′40″ N, 6°12′10″ E
Parent material	reworked loess (fluvial deposit during Pleistocene/Holocene)	cover layer of aeolian sands over loess
Elevation, m asl	93	44
Annual mean temperature, °C	9.5	10
Annual mean precipitation, mm	689	808
Climate	humid temperate	humid temperate
Textural class, %		
Sand	4	73
Silt	79	23
Clay	17	4
Clay minerals	70% illite, 12% kaolinite, 9% chlorite, 9% smectite	mainly illite
pH ($CaCl_2$)	6.5	5.4
Total organic C, g kg^{-1}	10	6
Field capacity, g cm^{-3}	37	27
Surface area (N_2), m^2 g^{-1}	10.3	1.9
Cation exchange capacity, $cmol_c$ kg^{-1}	11	5

pre-equilibration, 20 mL of the CsCl or $SrCl_2$ solution (using a soil/solution ratio of 1:5) were added to the centrifuged soil pellets and subsequently shaken. After equilibration, the soil suspensions were centrifuged at 2524 × *g* (polycarbonate tubes) or 1733 × *g* (glass tubes) at 20°C for 10 min. Following the OECD guidelines (Organisation for Economic Co-operation and Development, 2000), equilibration times of Cs^+ and Sr^{2+} were determined at 72 h for Cs^+ and 24 h for Sr^{2+}. After centrifugation, a 10-mL aliquot was collected to determine Cs^+ and Sr^{2+} concentrations by inductively couple plasma mass spectrometry using either an Elan 6100 (PerkinElmer) or an Agilent 7500 (Agilent Technologies). The isotopes ^{133}Cs, ^{86}Sr, ^{88}Sr, and ^{103}Rh were used as internal standards for quantification.

Classical Data Evaluation

Sorption isotherms were obtained by fitting the equilibrium data with the empirical Freundlich approach using OriginPro 8G (Version 8.0988, OriginLab Corporation):

$$C_s = K_f C_e^n$$

where C_s is the equilibrium concentration of Cs^+ or Sr^{2+} (mmol kg^{-1}) sorbed on the solid phase, and C_e is the equilibrium solution concentration (mmol L^{-1}). The Freundlich capacity parameter (K_f, $mmol^{1-n}\ L^n\ kg^{-1}$) reflects the sorption capacity, while the Freundlich exponent (n) reflects the nonlinearity of a sorption process. The parameters of the Freundlich isotherms are given in Table 2.

Modeling of the Sorption Process

First, measured sorption isotherms were analyzed with the Freundlich and Langmuir approach. However, these empirical approaches were not suitable to reproduce the measured sorption isotherms. Thus, the sorption process was analyzed with a sophisticated geochemical model using PHREEQC (Parkhurst and Appelo, 2013). Following Siegel and Bryan (2003), we simulated Cs^+ and Sr^{2+} sorption using different available cation exchange models and additionally a surface complexation model for Sr^{2+} (Fig. 1). This approach allowed the identification of the most suitable Cs^+ and Sr^{2+} sorption models and sorption parameters for various environmental conditions (soil type and amendment). After the suitable geochemical cation exchange and surface complexation models were identified, HP1 (Jacques and Šimůnek, 2005), which couples HYDRUS-1D (Šimůnek et al., 2013) with PHREEQC, was used to simulate RN transport along soil profiles. The reactions identified with PHREEQC were implemented into HP1. This approach allowed simulation of the complete suite of processes that occur within a lysimeter and affect RN transport: variable water flow, based on the Richards equation, evaporation, heat transport, and complex geochemical reactions.

Conceptual Cation Exchange Models

Our geochemical model accounts for cation exchange of Cs^+ and Sr^{2+} that occurs on OM and clay mineral surfaces, mostly controlled by the CEC of the soil. However, only two clay minerals of interest, illite and smectite, carry a permanent negative layer charge and are therefore relevant for Cs^+ and Sr^{2+}sorption. The permanent structural charge of the clay minerals caused by isomorphic substitution is fixed (Tan, 1993). Only for uncharged clay minerals can the surface charge vary with pH. However, all clay minerals show a pH-dependent charge at the edges (Tournassat et al., 2015). Thus, the impact of pH on cation exchange is mainly controlled by the OM content. Our simulations accounted for the influence of pH on the CEC by converting the potential CEC (measured at pH 7) into the effective CEC at the respective soil pH.

The potential CEC (CEC_{pot}) was determined according to the Mehlich (1942) $BaCl_2$ method. This revealed the maximum CEC available at pH 7 and 20°C. To account for the natural pH ranges in soil and pH changes due to amendment addition, the model used measured Cs^+ and Sr^{2+} concentrations to convert CEC_{pot} into effective CEC (CEC_{eff}), hence displaying the impact of pH on cation exchange. The differences between potential and effective CEC were analyzed using different cation exchange models: (i) a general cation exchange model (Model A) accounting for all colloids (OM and clay minerals) contributing to CEC; and (ii) cation exchange on illite only (Model B). Both cation exchange models are based on the Gaines–Thomas approach (Gaines and Thomas, 1953).

Table 2. Freundlich capacity parameter K_f and Freundlich linearity parameter n values of the Freundlich isotherms at 5°C and residual mean square (RMS) values.

Soil	Organic amendment	Cs^+			Sr^{2+}		
		K_f	n	RMS	K_f	n	RMS
		$mmol^{1-n}\ L^n\ kg^{-1}$			$mmol^{1-n}\ L^n\ kg^{-1}$		
silty loam	–	13.32 ± 2.25†	0.76 ± 0.05	2.02	5.55 ± 0.77	0.85 ± 0.07	3.89
	biochar	26.01 ± 17.29	0.82 ± 0.19	21.14	5.16 ± 0.55	0.80 ± 0.06	2.00
	digestate	21.36 ± 12.23	0.85 ± 0.15	14.29	4.80 ± 0.31	0.85 ± 0.02	2.45
sandy loam	–	2.80 ± 0.10	0.49 ± 0.01	0.21	1.32 ± 0.10	0.84 ± 0.06	0.43
	biochar	3.42 ± 0.29	0.52 ± 0.03	0.75	1.52 ± 0.13	0.86 ± 0.08	0.70
	digestate	3.22 ± 0.42	0.49 ± 0.09	0.96	0.97 ± 0.02	0.80 ± 0.00	0.33

† Means ± standard errors.

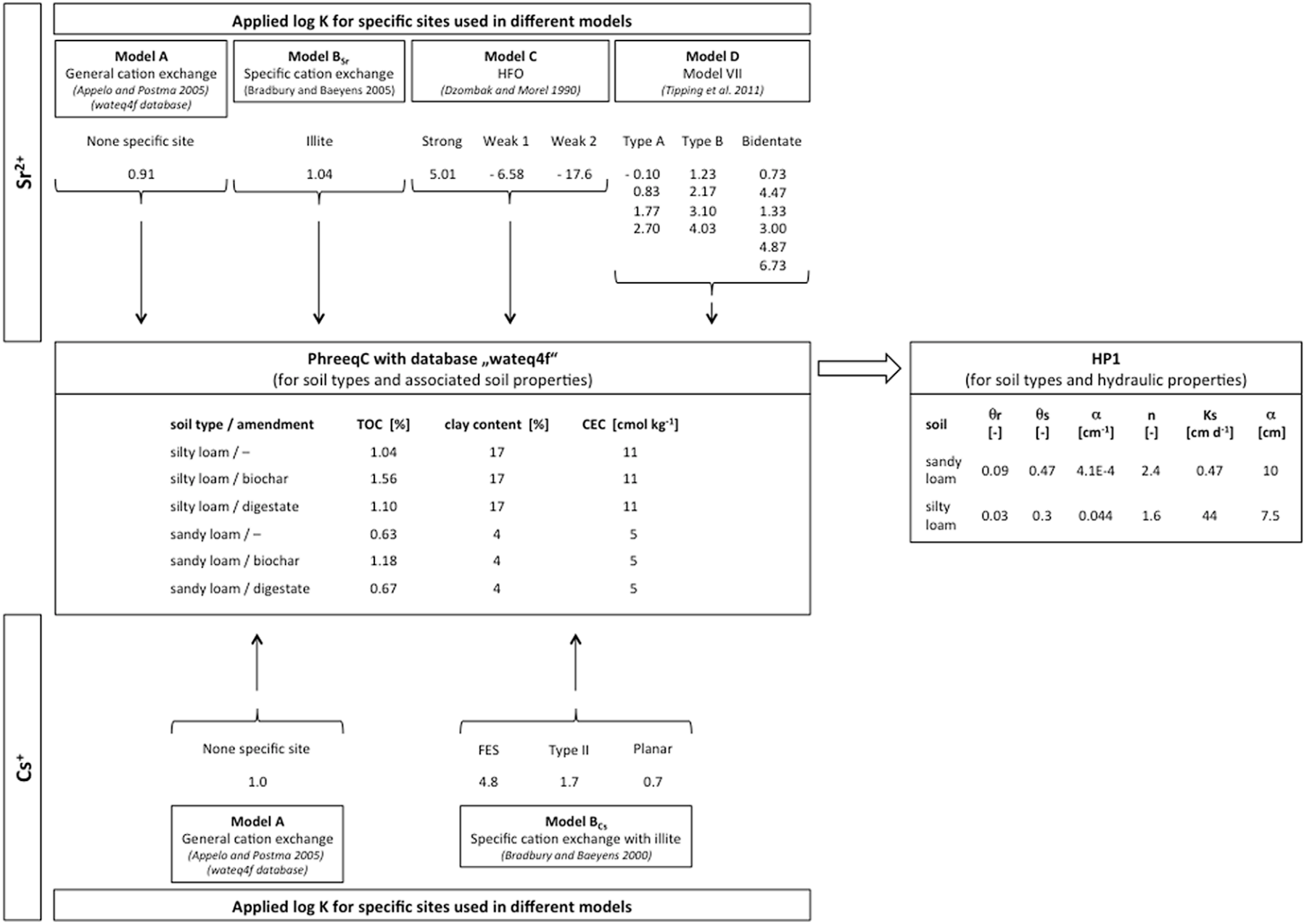

Fig. 1. Concept and strategy of Cs^{+} and Sr^{2+} sorption modeling approaches for silty and sandy loam soil types.

General cation exchange is simulated using the standard *wateq4f* database of PHREEQC (Appelo and Postma, 2005).

Highly selective cation exchange of Cs^+ on illite (Model B_{Cs}) is implemented according to Bradbury and Baeyens (2000) using three different exchange site types: frayed edge sites (FES), Type II sites, and planar sites, with a distribution of 0.25, 20.00, and 79.75%, respectively. Based on the illite content of the soils, an initial number of the different site types can thus be calculated and adjusted later during model calibration. Equilibrium distribution coefficients of Cs^+ and K^+, the main competing cation, were obtained according to Bradbury and Baeyens (2000).

Specific cation exchange of Sr^{2+} on illite (Model B_{Sr}) is implemented according to Bradbury and Baeyens (2005) with a CEC of 23 $cmol_c\ kg^{-1}$ for illite and an equilibrium constant of 1.04 using an identical selectivity for Sr^{2+}, Ca^{2+}, and Mg^{2+}. The specific $CEC_{eff,illite}$ was later subtracted from the adjusted CEC_{eff} to differentiate between the CEC contribution by OM and illite.

Model parameters were calculated for experimental data measured at 5°C. To account for the temperature dependence of sorption, the change in enthalpy (ΔH) values were adjusted based on experimental data obtained at 20 and 35°C (see supplemental material). The temperature dependence of Cs^+ and Sr^{2+} sorption was calculated by the Van't Hoff equation. Standard ΔH was adjusted to account for the temperature dependence of cation exchange. Temperature dependence of the surface complexation of Sr^{2+} was not considered because the effect was negligible (Karasyova et al., 1999).

Conceptual Surface Complexation Models

Currently, several conceptual surface complexation models have been published, e.g., (i)surface complexation on hydrous ferric oxides (HFO) (Dzombak and Morel, 1990), (ii) non-ideal competitive adsorption (NICA-Donnan model) (Kinniburgh et al., 1999), or (iii) the binding site type specific Model VII (Tipping et al., 2011). The most suitable models for our geochemical simulations were surface complexation on HFO, already available in PHREEQC, and Model VII, newly implemented into PHREEQC in this study, as both well-cited models account for geochemical processes and their concepts have already been successfully tested.

The Dzombak and Morel (1990) (Model C) model simulates surface complexation of Sr^{2+} on HFO based on available binding sites obtained from the amount of oxalate-extractable Fe.

Model VII by Tipping et al. (2011) accounts for the interaction of Sr^{2+} with fulvic and humic acids (Model D) and allows the specification of binding site types of humic substances, differentiated into mono- and bidentate sites. Monodentate sites consist of carboxyl (Type A) and phenol groups (Type B) (Tipping, 2002; Tipping et al., 2011). Bidentate sites (chelates) comprise monodentate sites located close together that allow bidentate binding of Sr^{2+}. This fraction of site types is accounted for by setting factor f to 0.5. Binding site types can be estimated from the TOC content. However, to account for the uncertainty of the measured TOC content, the number of sites was used as adjustable model parameter.

Furthermore, equilibrium constants were estimated applying default $\log K_{MA}$ values (monodentate sites Type A), while $\log K_{MB}$ (monodentate sites Type B) were calculated according to Tipping et al. (2011). The final $\log K_{MA}$ depended on the composition of Type A and B sites.

Surface complexation on OM only plays a minor role in Cs^+ sorption (Dumat et al., 1997; Lofts et al., 2002) and was not implemented for Cs^+.

Geochemical Model Calibration

All conceptual models (Fig. 1) were examined separately for their suitability to replicate the measured isotherms.

For Sr^{2+} sorption, the CEC_{eff} of the general cation exchange model (Model A) was adjusted first. Then, based on the illite content of the soil, $CEC_{eff,illite}$ was derived from the specific cation exchange model (Model B_{Sr}). This calibration strategy allowed the separation of total CEC_{eff} into fractions of variable (general cation model) and fixed (specific cation model) charges. Then, surface complexation model parameters (Models C and D) were adjusted by estimating the humic acid content.

Similarly, CEC_{eff} was obtained from Cs^+ isotherms by Models A and B_{Cs}. In addition to CEC_{eff} and $CEC_{eff,illite}$, equilibrium constants for specific cation exchange on illite were estimated. The equilibrium constant for K^+ (Bradbury and Baeyens, 2000) was kept constant.

Synthetic Long-Term and Field-Scale Cesium and Strontium Transport Experiment

Transport of $^{137}Cs^+$ and $^{90}Sr^{2+}$ through the two investigated agricultural soils (silty loam and sandy loam) was simulated using HP1 for a one-dimensional lysimeter setup. The one-dimensional model was discretized into 101 nodes with an initial temperature of 25°C and an initial water saturation of 0.1. Simulation time was 3 yr. The lysimeter soils were treated as one homogenous soil layer consisting of the respective soils used in the modeled batch experiments. Hydraulic and thermal boundary conditions were imposed based on time series of precipitation, evaporation, and temperature measured between 2008 and 2011 at the meteorological station of the Forschungszentrum Jülich GmbH, Germany (Engelhardt et al., 2015). Flow and transport parameters of the top layer (40-cm depth) of the two arable soils, hydraulic, atmospheric, as well as thermal boundary conditions stem from a long-term lysimeter simulation (Engelhardt et al., 2015).

The predictive simulations assumed that precipitation infiltrated at the top of the lysimeter with (i) a composition typical for a humid climate (0.38 $mg\ L^{-1}$ K^+, 0.31 $mg\ L^{-1}$ Ca^{2+}, 0.04 $mg\ L^{-1}$ Mg^{2+}, and pH 6) and (ii) fallout precipitation with an additional amount of 2,740,000 $Bq\ kg^{-1}$ for $^{137}Cs^+$ (8.56×10^{-4} $mg\ kg^{-1}$) or 36,000 $Bq\ kg^{-1}$ for $^{90}Sr^{2+}$ (7.06×10^{-6} $mg\ kg^{-1}$) as measured at distances of 4 to 5 km from the nuclear power plants in Chernobyl and Fukushima (Steinhauser et al., 2014). The fallout precipitation concentration including $^{137}Cs^+$ or $^{90}Sr^{2+}$ was applied as the initial concentration of the first precipitation event. Due to high specific

activities of $^{137}Cs^{+}$ (3200 GBq g^{-1}) and $^{90}Sr^{2+}$ (5100 GBq g^{-1}), the RN mass concentrations applied in the forward model were much lower than the concentrations in the batch experiments.

The complete suite of the geochemical reaction network including the specific parameters identified by calibrating the batch experiments was implemented into the one-dimensional flow and transport model. The forward model accounts for (i) the transient hydrogeochemical interaction of Cs^{+} and Sr^{2+} with the dissolved chemical soil water compounds, (ii) the soil type, (iii) heterogeneities in the soil hydraulic parameters (e.g., preferential flow paths), (iv) variably saturated conditions, and (v) transient climatic conditions (i.e., transient heat and water fluxes).

For the interpretation of the predicted leaching risk, threshold values for Cs^{+} and Sr^{2+} in soils according to the German radiation protection bylaw (Bundesministerium der Justiz und für Verbraucherschutz, 2016) were used as the lower cutoff boundary where soil contamination is negligible or nil. These threshold values were 3×10^{-2} Bq $g^{-1} = 0.7 \times 10^{-13}$ mol kg^{-1} for $^{137}Cs^{+}$ and 1×10^{-3} Bq $g^{-1} = 2.2 \times 10^{-15}$ mol kg^{-1} for $^{90}Sr^{2+}$.

Results and Discussion

Freundlich Sorption Parameters from Batch Experiments

For low concentrations (<0.5 mmol L^{-1}), the Freundlich sorption model was able to reproduce measured sorption isotherms for both RNs. However, the Freundlich model could not explain sorption at higher concentrations (Fig. 2). The Freundlich exponent n ranged between 0.49 and 0.85 for Cs^{+} and between 0.80 and 0.86 for Sr^{2+} (Table 2). Hence, all sorption isotherms displayed an L-type Freundlich sorption isotherm, indicating decreasing bonding energies with increasing amounts of sorbed RNs. This is usually attributed to a decreasing number of available sorption sites. This effect is much less pronounced in the sorption isotherms of Sr^{2+}, which display more linear sorption behavior. The Freundlich distribution coefficients (K_f) for both types of RN changed with respect to soil texture and were lower for the soil with higher sand content.

Both amendments were expected to increase both OM content and the CEC of the soils. As is apparent from Fig. 1, the amended soils showed increased TOC contents. As expected, the biochar amendment was less degradable than the digestate, and after 6 mo of incubation (prior to the sorption experiments), the biochar-amended silty loam and sandy loam had TOC contents that were 50 and 87% higher, respectively, than the unamended soils. The TOC contents of the digestate-amended soils increased by only 6% for both soil types. In both soil types, however, the biochar amendment decreased the measured CEC_{pot} (by 2.5 and 5.9%, respectively), which indicates a blocking of sites. Digestate amendment slightly decreased the CEC_{pot} in the silty loam (1.8%), while it induced a small increase in CEC_{pot} in the sandy loam (3.8%). From these soil characteristics it can be expected that Cs^{+} sorption is reduced with reduced CEC and that Sr^{2+} sorption increases as more OM sites are available. Measured

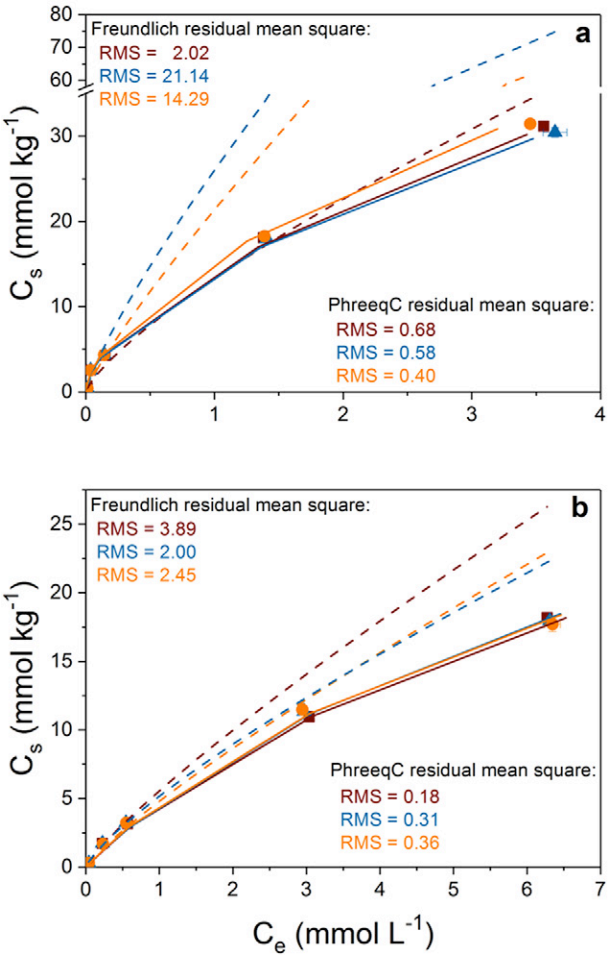

Fig. 2. Measured sorption data (symbols) of (a) Cs^{+} and (b) Sr^{2+} sorption dynamics at 5°C in silty loam fitted with the empirical Freundlich model (dashed lines) and modeled with PHREEQC (solid lines) (red = unamended soils, blue = biochar amended, orange = digestate amended). Data represent mean ± one standard deviation (n = 3).

sorption data in the silty loam show that sorption is only slightly influenced, with no clear trend. In the sandy loam, however, biochar induced an increased Cs^{+} sorption, while digestate reduced sorption. While both organic amendments probably block mineral sorption sites, biochar compensated for this through its large surface area. The Sr^{2+} sorption in the silty loam was even less affected by amendments, but in the sandy loam biochar increased sorption while digestate reduced it. The increase in Sr^{2+} sorption in this case can be attributed to the increase in OM. The increase in the OM content through the digestate, however, had an adverse effect and reduced Sr^{2+} sorption. In this case, the blocking of sorption sites seems to outweigh the gain in new sorption sites.

The K_f values from the Freundlich fits were not in line with our expectation. At 5°C, the Cs^{+} sorption seemingly increased in both soil types for both amendments, while Sr^{2+} sorption was reduced except for the biochar-amended sandy loam (Table 2). This is mainly explained by the bad fit of the measured data, as seen in Fig. 2. Hence, the Freundlich fit did not permit a sensible

interpretation of the sorption data. Even the better fit of the Sr^{2+} sorption data (Fig. 2b) did not allow a detailed interpretation because K_f and n are lumped parameters.

Key Processes of Cesium and Strontium Sorption Identified by Geochemical Modeling

Unlike the empirical Freundlich model, hydrogeochemical simulation of the sorption processes generated a good fit across the whole concentration range (Fig. 2 and Supplemental Fig. S2 and S3).

The simulations identified cation exchange on illite for low Cs^+ concentrations as the dominant sorption process (Fig. 3a–3c and 4a–4c), which is in line with the results of Bergaoui et al. (2005), who found that illite is highly selective for Cs^+. The most important factor for the Cs^+ sorption pattern on illite was the Cs^+ concentration driving the selection of the site types. Similar to the results of Bergaoui et al. (2005), our simulations identified highly selective FES as dominant sorption sites at low Cs^+ concentrations, while at high concentrations less affine site types constituted the major sorption partners. Frayed edge sites are known to strongly bind and immobilize Cs^+ for longer periods than planar sites (Fuller et al., 2015). Cesium bound to planar sites is easily exchanged by competing ions (Dyer et al., 2000). Hence, at low Cs^+ concentrations, the number of FES is especially important because sorption of Cs^+ is less reversible. Further, the amount of Cs^+ sorbed on FES is neither available to plants nor prone to leaching.

In addition to illite, the OM content is a further key factor for the soil CEC (Giannakopoulou et al., 2007). For Cs^+, an increasing OM content reduces the sorption capacity of illite due to the formation of organo-clay complexes blocking sorption sites. This coating process is especially important for trace amounts of Cs^+ (Staunton et al., 2002).

For the whole Sr^{2+} concentration range, undefined cation exchange was identified as the dominant sorption process in all soil types. In silty loam and sandy loam, 90 and 75%, respectively, of Sr^{2+} was bound by general cation exchange and specific cation exchange, corresponding well with the results of Sysoeva et al. (2005) (Fig. 3d–3f and 4d–4f). Surface complexation on HFO (Model C) was not significant in any soil. However, surface complexation of OM (Model D) was the second most important Sr^{2+} sorption process. Simulations showed that, similar to the results of Skipperud and Salbu (2015), 10% (silty loam) to 30% (sandy loam) of Sr^{2+} was bound by surface complexation. Therefore, the OM content is a key parameter that directly influences Sr^{2+} sorption via surface complexation, a process reducing Sr^{2+} availability to plants (Van Bergeijk et al., 1992). However, only humic acid sites are relevant to surface complexation, while complexation of fulvic acids is less important due to the high solubility of the latter (Skipperud and Salbu, 2015). In contrast to Cs^+, for Sr^{2+} neither cation exchange nor surface complexation was affected by the Sr^{2+} concentration, and the relative contributions of the different sorption processes, although different in size among the different soil types, remained quite stable across the whole concentration range.

Factors Influencing Cesium and Strontium Sorption as Identified by Geochemical Modeling

Soil Types

Highly selective cation exchange on illite (Model B_{Cs}) was the key process of Cs^+ sorption (Fig. 2a and Supplemental Fig. S1). For low concentrations (up to 1 mmol L^{-1},) 85 to >95% of Cs^+ was bound to illite in all soil types (Fig. 3a and 4a). With increasing concentration, this proportion decreased to <50% (silty loam) and <65% (sandy loam) because of the increasing influence of general cation exchange. At concentrations of 0.1 mmol L^{-1}, approximately 19% (silty loam) and 7% (sandy loam) of Cs^+ sorbed on FES and approximately 16 and 18%, respectively, on Type II sites.

Cation exchange and surface complexation of OM enabled Sr^{2+} sorption. Cation exchange depended not only on clay content but also on pH and humic acid content. Surface complexation on HFO is only significant at a soil pH above 7.5 (Sahai et al., 2000) and is therefore negligible. Furthermore, Missana et al. (2008) demonstrated by sorption experiments on smectite–illite clay mixtures that surface complexation of Sr^{2+} at the edges of clay minerals can be neglected.

General cation exchange (Model A) was the relevant Sr^{2+} sorption process for all soils, with fractions of sorbed Sr^{2+} >60% for silty loam and >50% for sandy loam (Fig. 3d and 4d). The model showed that illite was the second most important sorption partner in the silty loam. In contrast, OM was the second most important sorbent in the sandy loam. However, as the ratio between mono- and bidentate sites can only be estimated and the soil OM in the model is represented by the humic–fulvic-acid concept, the numerical results have to be judged carefully.

Organic Amendment

Generally, sorption differences between types of amendment were more pronounced in the sandy loam than the silty loam (Fig. 3b, 3c, 4b, and 4c).

Biochar amendment had no significant impact on Cs^+ sorption either in the silty loam (Fig. 3b) or the sandy loam (Fig. 4b). Similarly, digestate amendment on either the silty loam (Fig. 3c) or sandy loam (Fig. 4c) induced effects well below changes of 10% and could not be considered as significant. In all soils and treatments, the illite content remained the key factor for Cs^+ sorption.

All amendments influenced Sr^{2+} sorption more strongly than Cs^+ sorption (Fig. 3e, 3f, 4e, and 4f). Biochar-amended silty loam showed no significant changes in the relative contributions of sorption processes (Fig. 3e). However, in the sandy loam, biochar increased the surface complexation fraction by 16%, with a concurrent decrease in general CEC (Fig. 4e), as also observed by Nartey and Zhao (2014) and Trakal et al. (2011) and in line with our expectations (see above). Although the overall experimental Sr^{2+} sorption in the silty loam was not influenced by the addition of digestate (Supplemental Fig. S3), geochemical modeling revealed

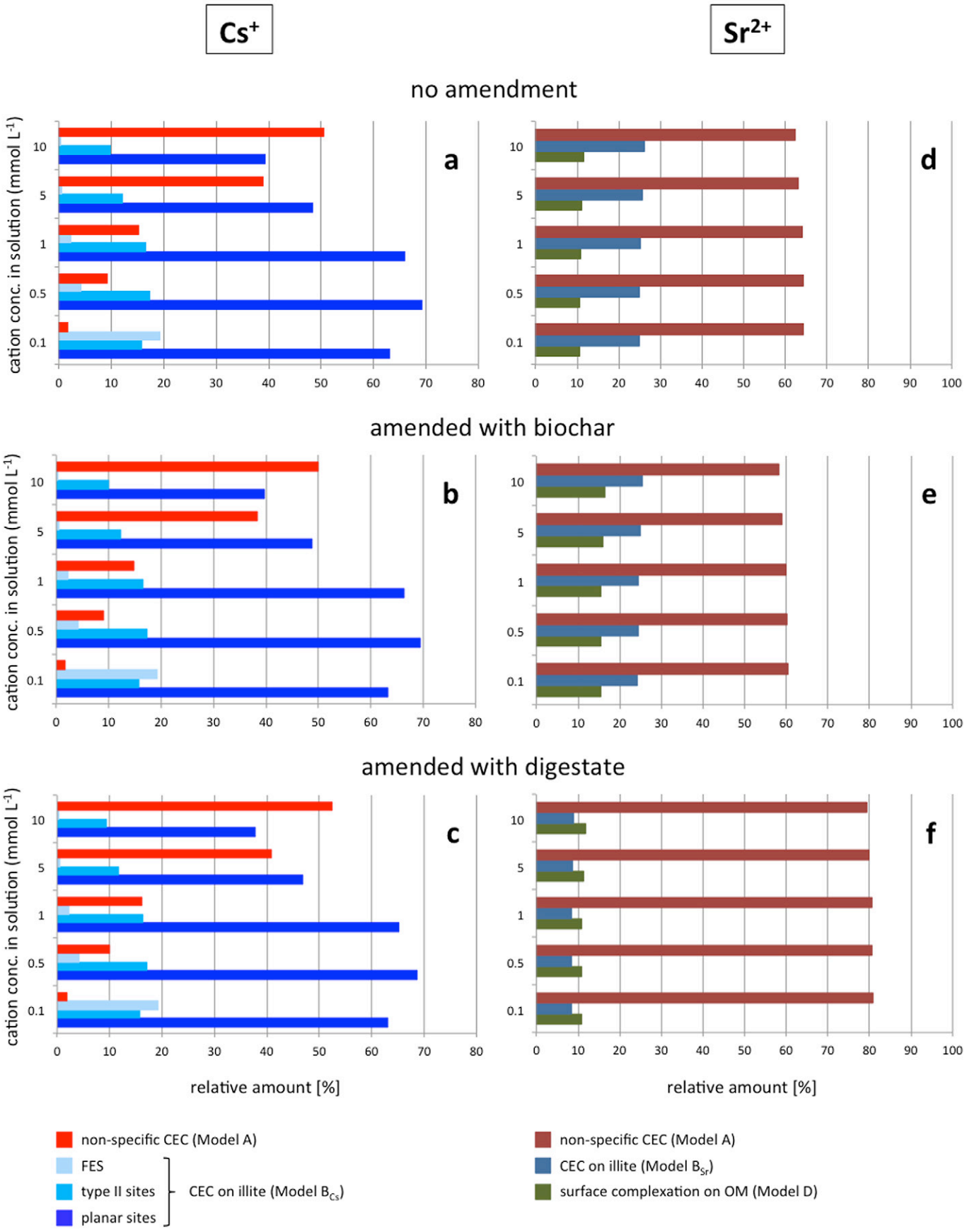

Fig. 3. Relative fractions of sorption processes at 5°C of (a–c) Cs^+ and (d–f) Sr^{2+} in silty loam without amendment (a and d), amended with biochar (b and e), and amended with digestate (c and f); CEC, cation exchange capacity; FES, frayed edge sites; OM, organic matter.

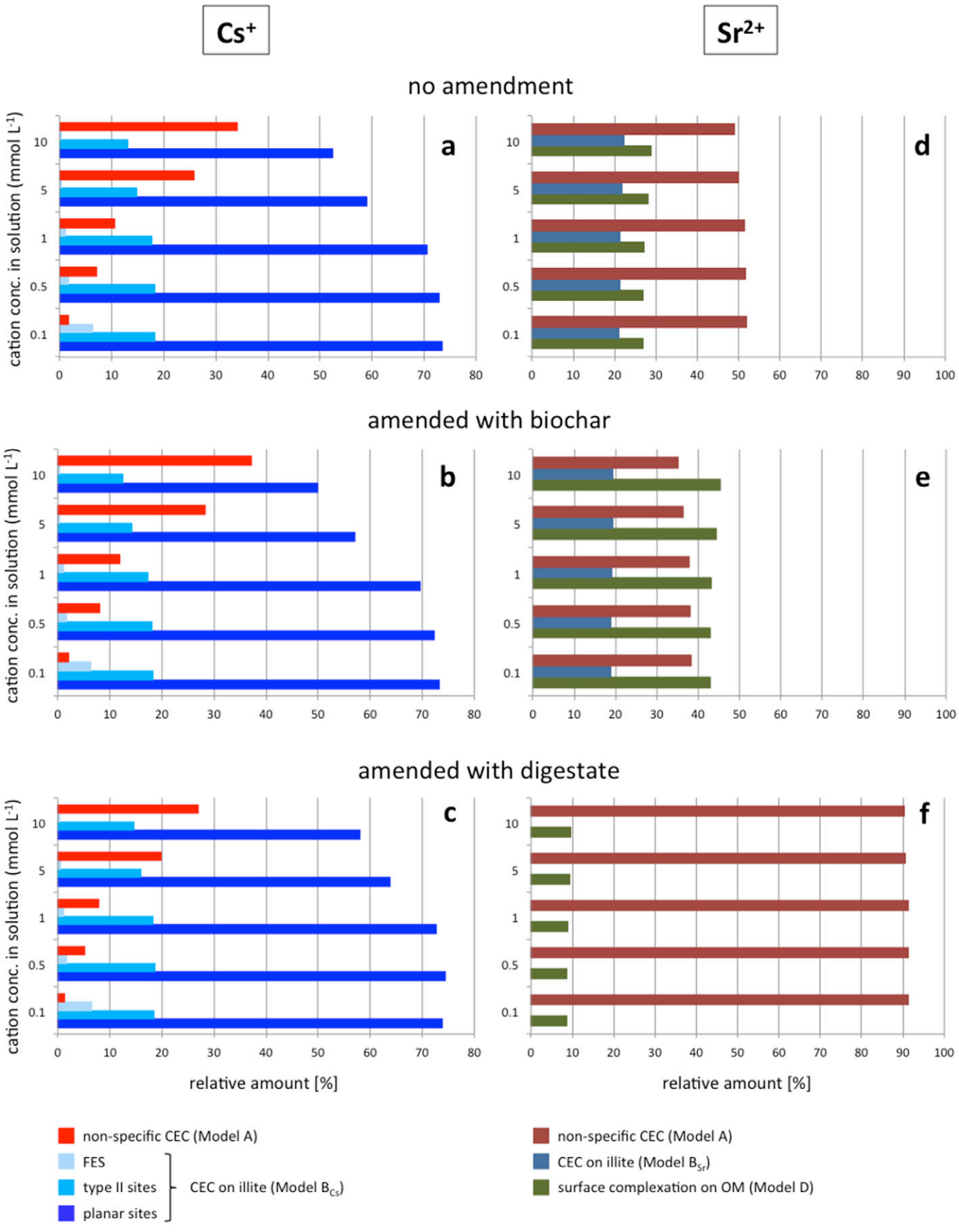

Fig. 4. Relative fractions of sorption processes at 5°C of (a–c) Cs^+ and (d–f) Sr^{2+} in sandy loam without amendment (a and d), amended with biochar (b and e), and amended with digestate (c and f); CEC, cation exchange capacity; FES, frayed edge sites; OM, organic matter.

a pronounced change in the distribution of the contributing sorption processes: sorption on illite decreased, while general cation exchange increased by 15% (Fig. 3f). Digestate amendment in the sandy loam had the most pronounced effect on Sr^{2+} sorption. Overall sorption of Sr^{2+} was reduced (Supplemental Fig. S3), which concurs with the modeled results showing that cation exchange on illite was reduced to 0, probably due to site blocking by OM. General cation exchange increased to >90% (Fig. 4f). This high impact of general cation exchange sites compared with cation exchange on illite increased the amount of plant-available Sr^{2+}, as also observed by Tan (1993).

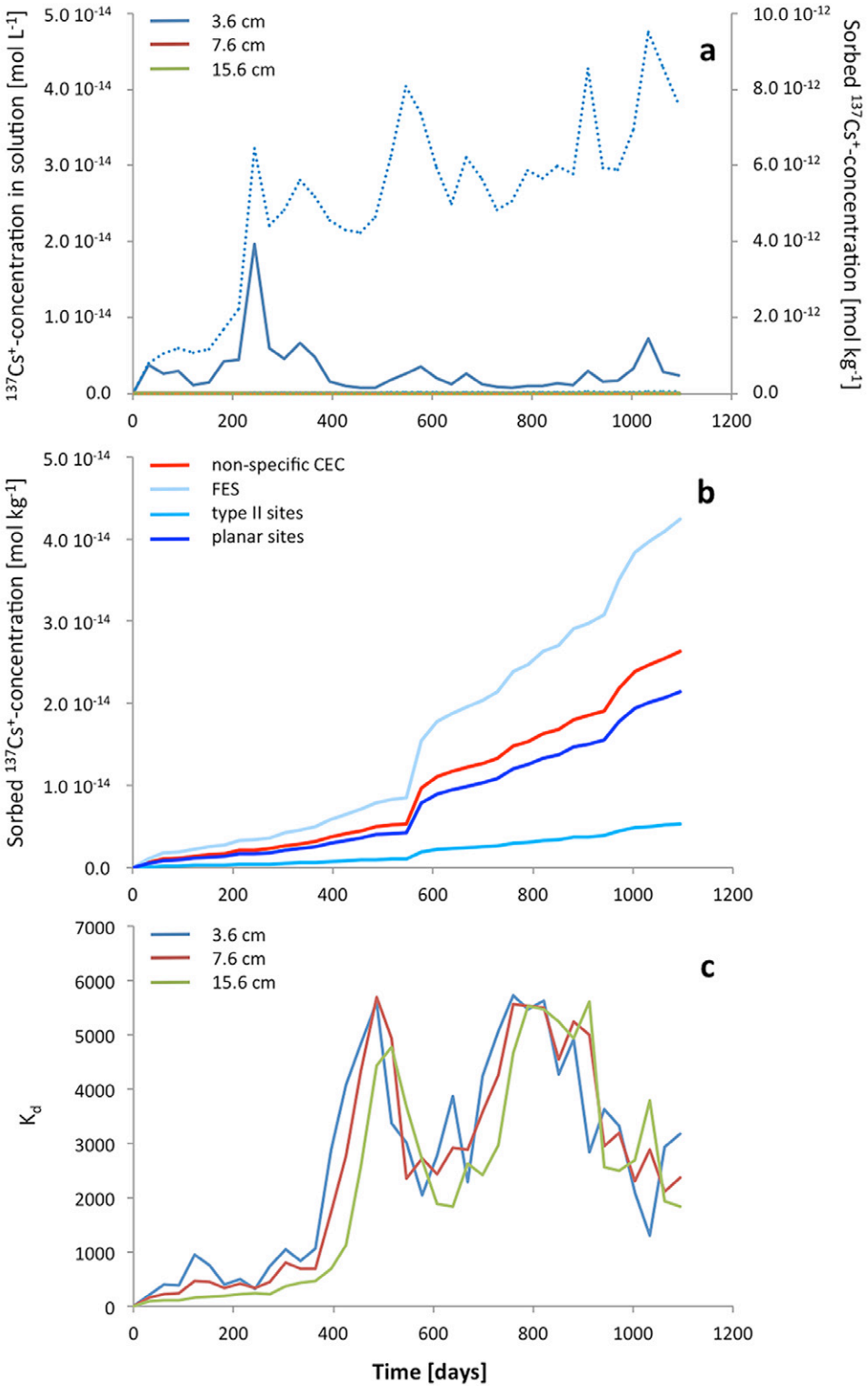

Fig. 5. (a) Depth distribution of $^{137}Cs^+$ concentrations in soil solution (solid lines) and in soil (dashed lines), (b) sorbed $^{137}Cs^+$ concentrations on different sorption site types at the 3.6-cm depth, and (c) distribution coefficients (K_d) of $^{137}Cs^+$ in different depth layers in modeled lysimeter experiments with unamended silty loam during a period of 3 yr; CEC, cation exchange capacity; FES, frayed edge sites.

Cesium-137 and Strontium-90 Leaching in Synthetic Lysimeter Experiment under Humid Climate

Forward modeling showed that after 3 yr, $^{137}Cs^+$ was transported to maximum depths of only 3.6 cm in the silty loam and 7.6 cm in the sandy loam (Fig. 5a and Supplemental Fig. S4a). In deeper parts of the soils (>4 cm in the silty loam and >8 cm in the sandy loam), $^{137}Cs^+$ concentrations were below the threshold value (3×10^{-2} Bq g^{-1} and 0.7×10^{-13} mol kg^{-1}).

At the 3.6-cm depth in the silty loam, the sorbed concentration slightly increased with time after breakthrough (240 d). The different site types contributed to the overall $^{137}Cs^+$ sorption process in the following decreasing order: FES > non-specific CEC > planar > Type II (Fig. 5b). In the sandy loam, sorbed $^{137}Cs^+$ increased for 40 d followed by a period of fluctuating concentrations (Supplemental Fig. S4a). The contribution of the site types was different from the silty loam, with FES > planar > non-specific CEC > Type II (Supplemental Fig. S5a). While in the silty loam none of the sites was saturated in the top 3.6 cm of soil during the 3-yr simulation, in the sandy loam the sites became saturated after approximately 400 d and hence Cs^+ was found in deeper soil layers. Possible explanations for the observed concentration fluctuations are the impact of temperature and water content, as both factors strongly vary in natural soils due to transient temperature as well as spatially and temporally

variable precipitation and evaporation fluxes. This fluctuating $^{137}Cs^{+}$ sorption was also apparent in the temporally variable K_d values (Fig. 5c and Supplemental Fig. S6a), which varied between 2000 and 6000 in the silty loam and between 1500 and 4000 in the sandy loam. At the field scale, the temporal and spatial variability of the key $^{137}Cs^{+}$ sorption processes was the dominant factor influencing the K_d values. Changes in the down- and upward water fluxes and hydraulic pattern had an additional effect on K_d values in the silty loam. The silty loam reached a higher maximum total sorption capacity due to a higher clay and OM content than the sandy loam. In both soils, the total values of sorbed $^{137}Cs^{+}$ were not affected by $^{137}Cs^{+}$ input concentrations.

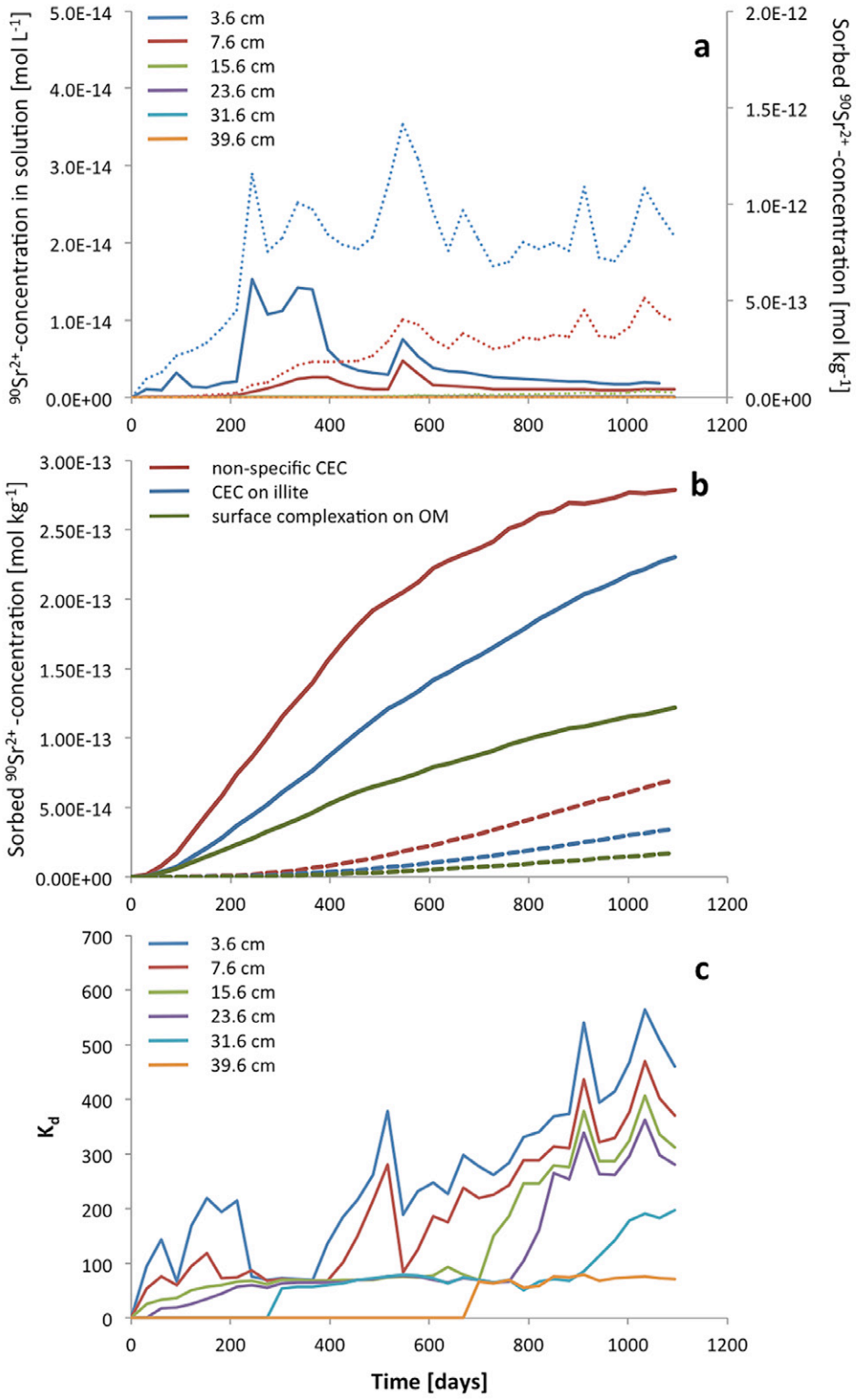

Fig. 6. (a) Depth distribution of $^{90}Sr^{2+}$ concentrations in soil solution (solid lines) and in soil (dashed lines), (b) sorbed $^{90}Sr^{2+}$ concentrations on different sorption site types at the 3.6-cm (solid lines) and 7.6-cm (dashed lines) depths, and (c) distribution coefficients (K_d) of $^{90}Sr^{2+}$ in different depth layers in modeled lysimeter experiments with unamended silty loam during a period of 3 yr; CEC, cation exchange capacity; FES, frayed edge sites; OM, organic matter.

Strontium-90 migrated to a depth of 15.6 cm in the silty loam (Fig. 6a). The $^{90}Sr^{2+}$ breakthrough (initial arrival) occurred at 3.6 cm after 200 d and at 7.6 cm after 500 d. In the sandy loam, $^{90}Sr^{2+}$ was detectable even at the 23.6-cm depth (Supplemental Fig. S4b), and breakthrough was observed at 3.6 cm after 40 d quickly followed by breakthroughs at levels 7.6 and 15.6 cm. In deeper parts of the soils (>16 cm in the silty loam and >24 cm in the sandy loam), the $^{90}Sr^{2+}$ concentration was below the threshold value of 2.2×10^{-15} mol kg^{-1} (1×10^{-3} Bq g^{-1}).

Concentrations in the soil solution showed similar fluctuations to those of $^{137}Cs^{+}$. In both the silty loam and sandy loam, the different site types contributed to the overall $^{90}Sr^{2+}$ sorption process in the following decreasing order of importance: CEC > CEC on illite > surface complexation on OM (Fig. 6b and Supplemental Fig. S5b). In the silty loam, none of the site types were saturated after 3 yr of simulation, while in the sandy loam all sites became quickly saturated at 3.6 cm and $^{90}Sr^{2+}$ migrated into deeper soil layers. At the 3.6-cm depth, competitive sorption between $^{90}Sr^{2+}$ and Ca^{2+} or Mg^{2+}, continuously infiltrating via rainwater, reduced $^{90}Sr^{2+}$ sorption. With longer simulation times, Ca^{2+} and Mg^{2+} displaced $^{90}Sr^{2+}$ from its exchange sites, and it then migrated to deeper soil layers, especially in the sandy loam. The K_d values and patterns for $^{90}Sr^{2+}$ were distinctively different from those obtained for $^{137}Cs^{+}$ (Fig. 6c and Supplemental Fig. S6b). At the

3.6-cm depth of the silty loam, the maximum K_d values ranged between 100 and 600, and in the sandy loam between 300 and 900. At the field scale, the relevant factors influencing the K_d values were temporal and spatial variability in the key $^{90}Sr^{2+}$sorption processes as well as competitive sorption, while changes in the hydraulic pattern and heat transport did not alter K_d values (see the supplemental material for more detailed information on temperature influence).

Our investigations used a physically based modeling tool that allows process-oriented prediction of the transport of $^{137}Cs^{+}$ and $^{90}Sr^{2+}$ radionuclides by accounting for complex sorption and ion exchange processes at the soil mineral and OM interfaces. It demonstrates that the investigated radionuclides are actually sorbed within the top soil layer, as observed after the Chernobyl nuclear accident (Ivanov et al., 1997).

Acknowledgments

This work was funded by the German Federal Ministry of Education and Research (BMBF) under Contract no. 02NUK015E, KVSF. We would like to thank Edward Tipping for his support with the implementation of the surface complexation processes into the geochemical model, Anne-Kathrin Nuffer for her assistance during the sorption experiments, and Andre Banning for several helpful discussions.

References

Appelo, C.A.J., and D. Postma. 2005. Geochemistry, groundwater and pollution. 2nd ed. CRC Press, Boca Raton, FL. doi:10.1201/9781439833544

Bergaoui, L., J.F. Lambert, and R. Prost. 2005. Cesium adsorption on soil clay: Macroscopic and spectroscopic measurements. Appl. Clay Sci. 29:23–29. doi:10.1016/j.clay.2004.09.002

Berns, A.E., H. Philipp, H.-D. Narres, P. Burauel, H. Vereecken, and W. Tappe. 2008. Effect of gamma-sterilization and autoclaving on soil organic matter structure as studied by solid state NMR, UV and fluorescence spectroscopy. Eur. J. Soil Sci. 59:540–550. doi:10.1111/j.1365-2389.2008.01016.x

Borchard, N., K. Prost, T. Kautz, A. Moeller, and J. Siemens. 2012. Sorption of copper (II) and sulphate to different biochars before and after composting with farmyard manure. Eur. J. Soil Sci. 63:399–409. doi:10.1111/J.1365-2389.2012.01446.X

Bradbury, M.H., and B. Baeyens. 2000. A generalised sorption model for the concentration dependent uptake of caesium by argillaceous rocks. J. Contam. Hydrol. 42:141–163. doi:10.1016/S0169-7722(99)00094-7

Bradbury, M.H., and B. Baeyens. 2005. Experimental and modelling investigations on Na-illite: Acid–base behaviour and the sorption of strontium, nickel, europium and uranyl. Tech. Rep. PSI-05-02. Paul Scherrer Inst., Villigen PSI, Switzerland.

Bundesministerium der Justiz und für Verbraucherschutz. 2016. Verordnung über den Schutz vor Schäden durch ionisierende Strahlen (Strahlenschutzverordnung vom 20. Juli 2001 (Bgbl. I s. 1714; 2002 i s. 1459), die zuletzt durch Artikel 8 des Gesetzes vom 26. Juli 2016 (Bgbl. I s. 1843) geändert worden ist). Bundesanzeiger Verlagsges., Köln, Germany.

Chamard, P., R.H. Velasco, M. Belli, G. Di Silvestro, G. Ingrao, and U. Sansone. 1993. Caesium-137 and strontium-90 distribution in a soil profile. Sci. Total Environ. 136:251–258. doi:10.1016/0048-9697(93)90313-U

Cornell, R.M. 1993. Adsorption of cesium on minerals: A review. J. Radioanal. Nucl. Chem. 171:483–500. doi:10.1007/BF02219872

de la Rosa, J.M., M. Paneque, A.Z. Miller, and H. Knicker. 2014. Relating physical and chemical properties of four different biochars and their application rate to biomass production of Lolium perenne on a Calcic Cambisol during a pot experiment of 79 days. Sci. Total Environ. 499:175–184. doi:10.1016/j.scitotenv.2014.08.025

Dumat, C., M.V. Cheshire, A.R. Fraser, C.A. Shand, and S. Staunton. 1997. The effect of removal of soil organic matter and iron on the adsorption of radiocaesium. Eur. J. Soil Sci. 48:675–683. doi:10.1111/j.1365-2389.1997.tb00567.x

Dumat, C., and S. Staunton. 1999. Reduced adsorption of caesium on clay minerals caused by various humic substances. J. Environ. Radioact. 46:187–200. doi:10.1016/S0265-931X(98)00125-8

Dyer, A., J.K.K. Chow, and I.M. Umar. 2000. The uptake of caesium and strontium radioisotopes onto clays. J. Mater. Chem. 10:2734–2740. doi:10.1039/b006662l

Dzombak, D.A., and F.M.M. Morel. 1990. Surface complexation modeling: Hydrous ferric oxide. John Wiley & Sons, New York.

Engelhardt, I., S. Sittig, J. Šimůnek, J. Groeneweg, T. Pütz, and H. Vereecken. 2015. Fate of the antibiotic sulfadiazine in natural soils: Experimental and numerical investigations. J. Contam. Hydrol. 177–178:30–42. doi:10.1016/j.jconhyd.2015.02.006

Fuller, A.J., S. Shaw, M.B. Ward, S.J. Haigh, J.F.W. Mosselmans, C.L. Peacock, et al. 2015. Caesium incorporation and retention in illite interlayers. Appl. Clay Sci. 108:128–134. doi:10.1016/j.clay.2015.02.008

Gaines, G.L., and H.C. Thomas. 1953. Adsorption studies on clay minerals: II. A formulation of the thermodynamics of exchange adsorption. J. Chem. Phys. 21:714–718. doi:10.1063/1.1698996

Garré, S., J. Köstel, T. Günther, M. Javaux, J. Vanderborght, and H. Vereecken. 2010. Comparison of heterogeneous transport processes observed with electrical resistivity tomography in two soils. Vadose Zone J. 9:336–349. doi:10.2136/vzj2009.0086

Giannakopoulou, F., C. Haidouti, A. Chronopoulou, and D. Gasparatos. 2007. Sorption behavior of cesium on various soils under different pH levels. J. Hazard. Mater. 149:553–556. doi:10.1016/j.jhazmat.2007.06.109

Goldberg, S., L.J. Criscenti, D.R. Turner, J.A. Davis, and K.J. Cantrell. 2007. Adsorption–desorption processes in subsurface reactive transport modeling. Vadose Zone J. 6:407–435. doi:10.2136/vzj2006.0085

Hamilton, T.F., R.E. Martinelli, S.R. Kehl, M.H.B. Hayes, I.J. Smith, S.K.G. Peters, et al. 2016. A preliminary assessment on the use of biochar as a soil additive for reducing soil-to-plant uptake of cesium isotopes in radioactively contaminated environments. J. Radioanal. Nucl. Chem. 307:2015–2020. doi:10.1007/s10967-015-4520-8

Hormann, V., and H.W. Fischer. 2013. Estimating the distribution of radionuclides in agricultural soils: Dependence on soil parameters. J. Environ. Radioact. 124:278–286. doi:10.1016/j.jenvrad.2013.06.010

Ivanov, Y.A., N. Lewyckyj, S.E. Levchuk, B.S. Prister, S.K. Firsakova, N.P. Arkhipov, et al. 1997. Migration of 137Cs and 90Sr from Chernobyl fallout in Ukrainian, Belarussian and Russian soils. J. Environ. Radioact. 35:1–21. doi:10.1016/S0265-931X(96)00036-7

Jacques, D., and J. Šimůnek. 2005. User manual of the multicomponent variably saturated flow and transport model HP1. Open Rep. SCK•CEN-BLG-998. SCK•CEN, Mol, Belgium.

Jacques, D., J. Šimůnek, D. Mallants, and M.Th. van Genuchten. 2006. Modelling uranium leaching from agricultural soils to groundwater as a criterion for comparison with complementary safety indicators. Mater. Res. Soc. Symp. Proc. 932:1057–1064. doi:10.1557/PROC-932-2.1

Karasyova, O.N., L.I. Ivanova, L.Z. Lakshtanova, and L. Lövgren. 1999. Strontium sorption on hematite at elevated temperatures. J. Colloid Interface Sci. 220:419–428. doi:10.1006/jcis.1999.6474

Kashparov, V.A., S.M. Lundin, S.I. Zvarych, V.I. Yoshchenko, S.E. Levchuk, Y.V. Khomutinin, et al. 2003. Territory contamination with the radionuclides representing the fuel component of Chernobyl fallout. Sci. Total Environ. 317:105–119. doi:10.1016/S0048-9697(03)00336-X

Kasteel, R., M. Burkhardt, S. Giesa, and H. Vereecken. 2005. Characterization of field tracer transport using high-resolution images. Vadose Zone J. 4:101–111. doi:10.2136/vzj2005.0101dup

Kinniburgh, D.G., W.H. van Riemsdijk, L.K. Koopal, M. Borkovec, M.F. Benedetti, and M.J. Avena. 1999. Ion binding to natural organic matter: Competition, heterogeneity, stoichiometry and thermodynamic consistency. Colloids Surf. A 151:147–166. doi:10.1016/S0927-7757(98)00637-2

Kleber, M. 2010. What is recalcitrant soil organic matter? Environ. Chem. 7:320–332. doi:10.1071/EN10006

Krouglov, S.V., A.S. Filipas, R.M. Alexakhin, and N.P. Arkhipov. 1997. Long-term study on the transfer of 137Cs and 90Sr from Chernobyl-contaminated soils to grain crops. J. Environ. Radioact. 34:267–286.

doi:10.1016/0265-931X(96)00043-4

Lehto, J. 2015. Sorption processes of radiocesium in soil and bedrock. Radiochim. Acta 103:213–218. doi:10.1515/ract-2014-2339

Lofts, S., E.W. Tipping, A.L. Sanchez, and B.A. Dodd. 2002. Modelling the role of humic acid in radiocaesium distribution in a British upland peat soil. J. Environ. Radioact. 61:133–147. doi:10.1016/S0265-931X(01)00118-7

Maes, N., S. Salah, C. Bruggeman, M. Aertsens, E. Martens, and L. Van Laer. 2012. Strontium retention and migration behaviour in boom clay. Ext. Rep. SCK•CEN-ER-197. SCK•CEN, Mol, Belgium.

Mehlich, A. 1942. Rapid estimation of base-exchange properties of soil. Soil Sci. 53:1–14. doi:10.1097/00010694-194201000-00001

Missana, T., M. Garcia-Gutierrez, and U. Alonso. 2008. Sorption of strontium onto illite/smectite mixed clays. Phys. Chem. Earth 33:S156–S162. doi:10.1016/j.pce.2008.10.020

Mukherjee, S., L. Weihermüller, W. Tappe, H. Vereecken, and P. Burauel. 2016. Microbial respiration of biochar- and digestate-based mixtures. Biol. Fertil. Soils 52:151–164. doi:10.1007/s00374-015-1060-x

Nartey, O.D., and B.W. Zhao. 2014. Biochar preparation, characterization, and adsorptive capacity and its effect on bioavailability of contaminants: An overview. Adv. Mater. Sci. Eng. doi:10.1155/2014/715398

Niedrée, B., A.E. Berns, H. Vereecken, and P. Burauel. 2013. Do Chernobyl-like contaminations with 137Cs and 90Sr affect the microbial community, the fungal biomass and the composition of soil organic matter in soil? J. Environ. Radioact. 118:21–29. doi:10.1016/j.jenvrad.2012.11.007

Nilsson, K.K., B.S. Jensen, and L. Carlsen. 1985. The migration chemistry of strontium. Eur. Appl. Res. Rep., Nucl. Sci. Technol. Sect. 7:149–200.

Novotny, E.H., C.M.B.D. Maia, M.T.M. Carvalho, and B.E. Madari. 2015. Biochar: Pyrogenic carbon for agricultural use—A critical review. Rev. Bras. Cienc. Solo 39:321–344. doi:10.1590/01000683rbcs20140818

Organisation for Economic Co-operation and Development. 2000. OECD guideline for the testing of chemicals—Test no. 106: Adsorption–desorption using a batch equilibrium method. OECD Publ., Paris.

Organisation for Economic Co-operation and Development/Nuclear Energy Agency. 2012. Thermodynamic sorption modelling in support of radioactive waste disposal safety cases: NEA Sorption Project Phase III. OECD Publ., Paris. doi:10.1787/9789264177826-en.

Parkhurst, D.L., and C.A.J. Appelo. 2013. Description of input and examples for PHREEQC version 3: A computer program for speciation, batch-reaction, one-dimensional transport, and inverse geochemical calculations. Techniques and Methods 6–A43. USGS, Denver, CO.

Payne, T.E., V. Brendler, M. Ochs, B. Baeyens, P.L. Brown, J.A. Davis, et al. 2013. Guidelines for thermodynamic sorption modelling in the context of radioactive waste disposal. Environ. Modell. Softw. 42:143–156. doi:10.1016/j.envsoft.2013.01.002

Piqué, A., D. Arcos, F. Grandia, J. Molinero, L. Duro, and S. Berglund. 2013. Conceptual and numerical modeling of radionuclide transport and retention in near-surface systems. Ambio 42:476–487. doi:10.1007/s13280-013-0399-1

Prost, K., N. Borchard, J. Siemens, T. Kautz, J.-M. Séquaris, A. Möller, and W. Amelung. 2013. Biochar affected by composting with farmyard manure. J. Environ. Qual. 42:164–172. doi:10.2134/jeq2012.0064

Sahai, N., S.A. Carroll, S. Roberts, and P.A. O'Day. 2000. X-ray absorption spectroscopy of strontium(II) coordination: II. Sorption and precipitation at kaolinite, amorphous silica, and goethite surfaces. J. Colloid Interface Sci. 222:198–212. doi:10.1006/jcis.1999.6562

Sanchez, A.L., W.R. Schell, and E.D. Thomas. 1988. Interactions of 57Co, 85Sr and 137Cs with peat under acidic precipitation conditions. Health Phys. 54:317–322. doi:10.1097/00004032-198803000-00009

Scotti, R., G. Bonanomi, R. Scelza, A. Zoina, and M.A. Rao. 2015. Organic amendments as sustainable tool to recovery fertility in intensive agricultural systems. J. Soil Sci. Plant Nutr. 15:333–352.

Siegel, M.D., and C.R. Bryan. 2003. Environmental geochemistry of radioactive contamination. Treatise Geochem. 9:205–262.

Šimůnek, J., M. Šejna, H. Saito, and M.Th. van Genuchten. 2013. The HYDRUS-1D software package for simulating the movement of water, heat, and multiple solutes in variably saturated media, Version 4.17. HYDRUS Softw. Ser. 3. Dep. of Environ. Sci., Univ. of California, Riverside.

Skipperud, L., and B. Salbu. 2015. Sequential extraction as a tool for mobility studies of radionuclides and metals in soils and sediments. Radiochim. Acta 103:187–197. doi:10.1515/ract-2014-2342

Staunton, S., C. Dumat, and A. Zsolnay. 2002. Possible role of organic matter in radiocaesium adsorption in soils. J. Environ. Radioact. 58:163–173. doi:10.1016/S0265-931X(01)00064-9

Staunton, S., and P. Levacic. 1999. Cs adsorption on the clay-sized fraction of various soils: Effect of organic matter destruction and charge compensating cation. J. Environ. Radioact. 45:161–172. doi:10.1016/S0265-931X(98)00100-3

Steinhauser, G., A. Brandl, and T.E. Johnson. 2014. Comparison of the Chernobyl and Fukushima nuclear accidents: A review of the environmental impacts. Sci. Total Environ. 470–471:800–817 [erratum: 48:575]. doi:10.1016/j.scitotenv.2013.10.029

Sysoeva, A.A., I.V. Konopleva, and N.I. Sanzharova. 2005. Bioavailability of radiostrontium in soil: Experimental study and modeling. J. Environ. Radioact. 81:269–282. doi:10.1016/j.jenvrad.2004.01.040

Tambone, F., F. Adani, G. Gigliotti, D. Volpe, C. Fabbri, and M.R. Provenzano. 2013. Organic matter characterization during the anaerobic digestion of different biomasses by means of CPMAS 13C NMR spectroscopy. Biomass Bioenergy 48:111–120. doi:10.1016/j.biombioe.2012.11.006

Tan, K.H. 1993. Principles of soil chemistry. 2nd ed. Marcel Dekker, New York.

Tipping, E. 2002. Cation binding by humic substances. Cambridge Environ. Chem. Ser. 12. Cambridge Univ. Press, Cambridge, UK. doi:10.1017/CBO9780511535598

Tipping, E., S. Lofts, and J.E. Sonke. 2011. Humic Ion-Binding Model VII: A revised parameterisation of cation-binding by humic substances. Environ. Chem. 8:225–235. doi:10.1071/EN11016

Tournassat, C., C.I. Steefel, I.C. Bourg, and F. Bergaya, editors. 2015. Natural and engineered clay barriers. Dev. Clay Sci. 6. Elsevier, Amsterdam.

Trakal, L., M. Komárek, J. Száková, V. Zemanová, and P. Tlustoš. 2011. Biochar application to metal-contaminated soil: Evaluating of Cd, Cu, Pb and Zn sorption behavior using single- and multi-element sorption experiment. Plant Soil Environ. 57:372–380. doi:10.17221/155/2011-PSE

UN Scientific Committee on the Effects of Atomic Radiation. 1996. Sources and effects of ionizing radiation. United Nations, New York.

Van Bergeijk, K.E., H. Noordijk, J. Lembrechts, and M.J. Frissel. 1992. Influence of pH, soil type and soil organic matter content on soil-to-plant transfer of radiocesium and -strontium as analyzed by a non-parametric method. J. Environ. Radioact. 15:265–276. doi:10.1016/0265-931X(92)90062-X

Wang, G., and S. Staunton. 2005. Evolution of Sr distribution coefficient as a function of time, incubation conditions and measurement technique. J. Environ. Radioact. 81:173–185. doi:10.1016/j.jenvrad.2004.01.034